400 W Yb:YAG Innoslab fs-amplifier

P. Russbueldt[1,*], T. Mans[1], G. Rotarius[1], J. Weitenberg[2], H.D. Hoffmann[1] and R. Poprawe[1,2]

[1]*Fraunhofer Institute for Laser Technology, Steinbachstr. 15, 52074 Aachen, Germany*
[2]*Chair for Laser Technology RWTH Aachen, Steinbachstr. 15, 52074 Aachen, Germany*
*Corresponding author: *Peter.Russbueldt@ilt.fraunhofer.de*

Abstract: The Innoslab design, already established for neodymium doped laser crystals, was applied to ytterbium doped laser materials. Recent progresses in brightness of high power diode lasers facilitate efficient pumping of quasi-three-level laser materials. Innoslab amplifiers are compared to competing thin-disk and fiber fs-amplifiers. A compact diode-pumped Yb:YAG Innoslab fs-oscillator-amplifier system, scalable to the kilowatt range, was realized. Numerical simulations result in conditions for high efficiency and beam quality. Nearly transform and diffraction limited 680 fs pulses at 400 W average output power and 76 MHz repetition rate without using CPA technology have been achieved at room temperature so far.

OCIS codes: (140.3280) Laser amplifiers; (140.3615) Lasers, ytterbium; (140.7090) Ultrafast lasers

References and links

1. T. Südmeyer, S. V. Marchese, S. Hashimoto, C. R. E. Baer, G. Gingras, B. Witzel, and U. Keller, "Femtosecond laser oscillators for high-field science," Nat. Photon. **2**, 599-604 (2008).
2. K.-H. Hong, A. Siddiqui, J. Moses, J. Gopinath, J. Hybl, F. Ö. Ilday, T. Y. Fan, and F. X. Kärtner, "Generation of 287 W, 5.5 ps pulses at 78 MHz repetition rate from a cryogenically cooled Yb:YAG amplifier seeded by a fiber chirped-pulse amplification system," Opt. Lett. **33**, 2473-2475 (2008).
3. A. A. Kaminski, "Laser Crystals, Their Physics and Properties," 2nd Edition, Series in Optical Science **14**, Springer, Berlin/Heidelberg (1990).
4. L. D. DeLoach, S. A. Payne, L. L. Chase, L. K. Smith, L. Kway, and W. F. Krupke, "Evaluation of Absorption and Emission Properties of Yb^{3+} Doped Crystals for Laser Application," IEEE J. Quantum Electron. **29**, 1179-1191 (1993).
5. R. L. Aggarwal, D. J. Ripin, J. R. Ochoa, and T. Y. Fan, "Measurement of thermo-optic properties of $Y_3Al_5O_{12}$, $Lu_3Al_5O_{12}$, $YAlO_3$, $LiYF_4$, BaY_2F_8, $KGd(WO_4)_2$, and $KY(WO_4)_2$ laser crystals in the 80-300 K temperature range," J. Appl. Phys. **98** (2005).
6. R. G. Smith, "Optical Power handling capacity of low loss optical fibers as determined by stimulated Raman and Brillouin scattering," Appl. Opt. **11**, 2489-2494 (1972).
7. P. Maine, D. Strickland, P. Bado, M. Pessot, and G. Mourou, "Generation of ultra-high peak power pulses by chirped pulse amplification," IEEE J. Quantum Electron. **24**, 398-403 (1988).
8. F. Röser, J. Rothhard, B. Ortac, A. Liem, O. Schmidt, T. Schreiber, J. Limpert, and A. Tünnermann, "131 W 220 fs fiber laser system," Opt. Lett. **30**, 2754-2756 (2005).
9. A. Giesen, H. Hügel, A. Voss, K. Wittig, U. Brauch, and H. Opower, "Scalable Concept for Diode-Pumped High-Power Solid-State-Lasers," J. Appl. Phys. B **58**, 365-372 (1994).
10. A. Giesen and J. Speiser, "Fifteen Years of Work on Thin-Disk Lasers: Results and Scaling Laws," IEEE J. Sel. Top. Quantum Electron. **13**, 598-609 (2007).
11. M. Larionov, F. Butze, D. Nickel, and A. Giesen, "High-repetition-rate regenerative thin-disk amplifier with 116 µJ pulse energy and 250 fs pulse duration," Opt. Lett. **32**, 494-496 (2007).
12. C. Stolzenburg and A. Giesen, "Picosecond Regenerative Yb:YAG Thin Disk Amplifier at 200 kHz Repetition Rate and 62 W Output Power," Advanced Solid-State Photonics, OSA Tech. Digest, MA6 (2007).
13. K. Du, N. Wu, J. Xu, J. Giesekus, P. Loosen, and R. Poprawe, "Partially end-pumped Nd:YAG slab laser with a hybrid resonator," Opt. Lett. **23**, 370-372 (1998).
14. J. Giesekus, T. Mans, K.-M. Du, B. Braun, P. Loosen, and R. Poprawe, "High power diode end pumped slab MOPA system," International Conference on Lasers and Electrooptics, OSA Tech. Digest, CThI3 (2001).
15. B. Luther-Davies, V. Z. Kolev, M. J. Lederer, N. R. Madsen, A. V. Rode, J. Giesekus, K. M. Du, and M. Duering "Table-top 50-W laser system for ultra-fast laser ablation," J. Appl. Phys. A **00**, 1–5 (2004).
16. M. K. Davis, M. J. F. Digonnet, and R. H. Pantell, "Thermal effects in doped fibers," J. Lightwave Technol. **16**, 1013-1023 (1998).

#106480 - $15.00 USD Received 21 Jan 2009; revised 20 Apr 2009; accepted 20 Apr 2009; published 6 Jul 2009

17. D. C. Brown and H. J. Hoffmann, "Thermal, stress and thermo-optic effects in high average power double-clad fiber lasers," IEEE J. Quantum Electron. **37**, 207-217 (2001).
18. V. P. Gapontsev, "High Power Fiber Laser and its Application," International Conference "Laser Optics 2008," St. Petersburg (2008).
19. C. Schnitzler, M. Hoefer, J. Luttmann, D. Hoffmann, and R. Poprawe, "A cw kw-class diode end pumped Nd:YAG slab laser," International Conference on Lasers and Electrooptics, OSA Tech. Digest, CPDC2-1 (2002).
20. Y. Jeong, J. K. Sahu, D. N. Payne, and J. Nilsson, "Ytterbium-doped large-core fiber laser with 1.36 kW continuous-wave output power," Opt. Expr. **12**, 6088-6092 (2004).
21. K. Petermann, D. Fagundes-Peters, J. Johannsen, M. Mond, V. Peters, J. J. Romero, S. Kutovoi, J. Speiser, and A. Giesen, "Highly Yb-doped oxides for thin-disc lasers," J. of Crystal Growth **275**, 134-140 (2005).
22. P. Russbueldt, T. Mans, D. Hoffmann, and R. Poprawe, "High Power Yb:YAG Innoslab Fs-Amplifier," International Conference on Lasers and Electrooptics, OSA Tech. Digest, CTuK5 (2008).
23. F. Röser, T. Eidam, J. Rothard, O. Schmidt, D. N. Schimpf, J. Limpert, and A. Tünnermann, "Millijoule pulse energy high repetition rate femtosecond fiber chirped-pulse amplification system," Opt. Lett. **32**, 3495-3497 (2007).
24. S. Hädrich, T. Schreiber, T. Pertsch, J. Limpert, T. Peschel, R. Eberhardt, and A. Tünnermann, "Thermo-optical behavior of rare-earth-doped low-NA fibers in high power operation," Opt. Expr. **14**, 6091-6097 (2006).
25. G. Fibich and A. L. Gaeta, "Critical power for self-focussing in bulk media and in hollow waveguides," Opt. Lett. **25**, 335-337 (2000).
26. S, Chénais, F. Balembois, F. Druon, G. Lucas-Leclin, and P. Georges, "Thermal Lensing in Diode-Pumped Ytterbium Lasers – Part II: Evaluation of Quantum Efficiencies and Thermo-Optic Coefficients," IEEE J. Quantum Electron. **40**, 1235-1243 (2004).
27. T. Y. Fan, "Heat Generation in Nd:YAG and Yb:YAG," IEEE J. Quantum Electron. **29**, 1457-1459 (1993).
28. G. L. Bourdet, "Theoretical investigation of quasi-three-level longitudinally pumped continuous wave lasers," Appl. Opt. **39**, 966-971 (2000).
29. Q. Liu, X. Fu, M. Gong, and L. Huang, "Effects of temperature dependence of absorption coefficients in edge-pumped Yb:YAG slab lasers," J. Opt. Soc. Am. B **24**, 2081-2089 (2007).
30. D. S. Sumida and T. Y. Fan, "Emission Spectra and Fluorescence Lifetime Measurements of Yb:YAG as a Function of Temperature," OSA Proc. Adv. Solid-State Lasers, 100-102 (1994).

1. Introduction

To transfer femtosecond technology to industrial applications, laser sources of high average power and high repetition rate up to the MHz range are essential. These lasers have to combine sub picosecond pulse duration of ultrafast lasers and mean output power of high power lasers at nearly diffraction limited beam quality. Beside industrial applications these fs-lasers may be efficient tools at lower repetition rates for investigations in atomic, plasma and nuclear physics like XUV-generation or wakefield acceleration. Great effort has been made to develop such lasers. Mainly due to the ongoing improvements of power and brightness of commercially available laser diodes new solid state laser designs like thin-disk, fiber and partially pumped slab lasers (Innoslab) established beside rod lasers in the last decade.

Despite impressive progress in thin-disk laser technology for fs-oscillators [1] scaling to the multi 100 W level will most likely be done by master oscillator power amplifier (MOPA) configurations. This in particular holds for radiation of high beam quality at variable repetition rate or pulse train structure. This valuation is due to the fact that today's pulse energy of SESAM modelocked thin-disk oscillators relying on soliton like modelocking is limited. Scaling the pulse energy is done by very long cavities so far and there are still issues of instabilities and pulse break-ups due to the passive absorbers or the nonlinearity of air. Therefore only amplifiers are considered in the following. Furthermore special technologies unsuitable for industrial lasers like cryogenic cooling are not considered.

2. The Yb:Innoslab design in comparison with fiber and thin-disk lasers

2.1. Laser material

In case of fs-lasers the most basic decision is the choice of the laser medium. To generate or amplify ultrashort laser pulses with pulse durations below 1 ps, an amplification medium with a bandwidth much broader than the natural spectral line width is essential. In laser materials broadening of the emission bandwidth of the laser active ions takes place by phonon interactions and the Stark effect in the crystal lattice. Broadening of the gain bandwidth necessarily

#106480 - $15.00 USD Received 21 Jan 2009; revised 20 Apr 2009; accepted 20 Apr 2009; published 6 Jul 2009

reduces the gain cross section by the same factor. This is why cryo-cooling not only increases emission cross section and thermal conductivity but also reduces amplification bandwidth to values not suitable for sub-picosecond pulses [2].

For average powers beyond 100 W ytterbium doped media are established only. Main reason is the availability of high power and high brightness diode lasers in the $\lambda_p = 940 - 980$ nm wavelength range for pumping [3]. The emission cross section and upper state lifetime in the millisecond range is comparatively high i.e. the saturation intensity is low at sufficient bandwidth to support sub-picosecond pulses. This originates in the simple structure of few electronic states of the ytterbium ion just as the high quantum efficiency $\eta_q \approx 1$. The high Stokes efficiency at the lasing wavelength $\lambda \approx 1030$ nm and low waste power is accompanied by a thermally populated lower state of the laser transition. Because of the quasi-three-level energy scheme ytterbium doped materials absorb laser radiation below a specific pump intensity.

For efficient operation pump intensities throughout the gain volume in the order of the saturation intensity of the pump radiation $I_{sat}(\lambda_p)$ and an efficient heat removal from the gain volume are essential. These are the main requirements on a laser design employing ytterbium doped laser media. At average output powers above 100 W mainly Yb:YAG has been established among the crystal hosts. Of all commercially available ytterbium doped laser crystals it provides the highest emission cross section $\sigma_e = 2 \cdot 10^{-9}\,\mathrm{cm}^2$, the lowest saturation intensity $I_{sat}(\lambda_p) = 28\,\mathrm{kWcm}^{-2}$ [4] and the best optical quality at high heat conductivity $K = 8.6\,\mathrm{Wm}^{-1}\mathrm{K}^{-1}$ (2% doping) [5], but the lowest emission bandwidth $\Delta\lambda \approx 5$ nm (FWHM) as well [4]. Considering laser crystals Yb:YAG is the first choice for a high power laser design. Laser materials with broader emission bandwidth but lower emission cross section at comparable heat conductivity like the sesquioxides may be the second. Host materials like the tungstates showing a much broader emission of the ytterbium ions but low emission cross section and heat conduction are technically more demanding for a high average power laser design.

2.2. *Amplifier design*

Laser materials supporting short pulses require high pump intensities throughout the crystal. Good thermal management is essential to avoid failure by thermo-mechanical stress and to support nearly diffraction limited beam quality at high average power. Today three different basic designs fulfill these requirements in very different ways.

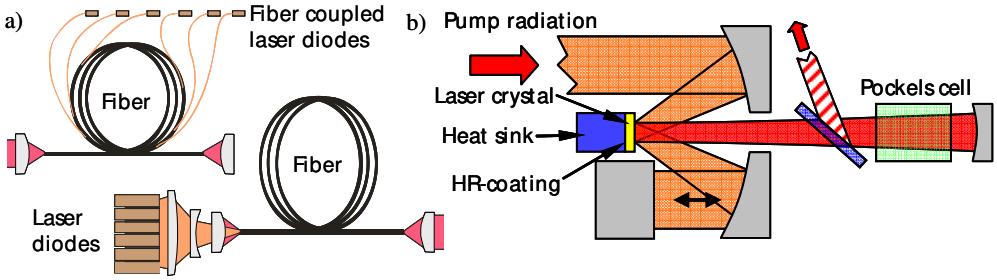

Fig. 1. Schematic setup of fiber amplifiers pumped by fused couplers and free space (a) and thin-disk amplifier (b)

A Fiber laser or amplifier consists of an active fiber, in- and output coupling and optional passive fiber components. At high output power the active fiber is cladding pumped. Usually the pump light is launched into the pump cladding of some 100 µm diameter by free space coupling into the end, fused combiners at the end or fused couplers along the fiber (Fig. 1(a)). The large surface of the several meters long active fiber eases heat removal. The laser radiation is completely confined in an active fiber core of some 10 µm diameter supporting fundamental mode operation. The long interaction length inside the fiber and the small core diameter makes efficient single path amplification with very high gain possible. Due to the small cross section of the active fiber core ultrashort laser pulses have to be amplified by chirped

#106480 - $15.00 USD Received 21 Jan 2009; revised 20 Apr 2009; accepted 20 Apr 2009; published 6 Jul 2009

pulse amplification in order to avoid nonlinear effects or damage by high peak power [6 - 8]. Stretcher and compressor are always free space components providing large cross sections.

A Thin-Disk Laser or amplifier is based on a thin active medium highly reflective coated and bonded to a heat sink on one side. If the thickness of the active medium of typically 100 µm is small in comparison to the incident beam diameter of typically some millimeters this active mirror is called a thin-disk Laser [9]. By the large diameter to thickness ratio the heat flow and thermal gradient inside the laser medium is approximately one-dimensional and nearly no thermal lens is established. The short distances inside the active medium to the heat sink allow for efficient heat removal. To achieve a sufficient absorption the pump radiation is folded many times (8 - 32x) back and forth through the disk by an imaging optics [10]. Thin-disks provide the largest possible diameter of the gain medium, but also the lowest single-pass gain. Therefore thin-disks are integrated in regenerative amplifiers to achieve enough gain for amplifying low power signals [11,12]. The low gain is system specific, as changes in dimensions or doping level will lead to a significant drop in performance (section 2.3). Thin disks can be used in multi-pass configurations too, but the low gain requires many passes to amplify an oscillator with typically not more than a few Watts of average output power. If multi 100 W signal sources become available, thin-disk lasers may be interesting for very high power booster amplifiers.

An Innoslab laser or amplifier consists of a longitudinally, partially pumped slab crystal [13]. Grinding of the mounting surfaces of the slab suppress parasitic oscillations across the line-shaped, homogeneously pumped cross section inside the crystal. The short distance between the pumped gain volume and the large cooled mounting surfaces allow for efficient heat removal. For cw-pumping, the thickness of the slab is in the order of $d \approx 1\,\mathrm{mm}$. One-dimensional heat flow establishes a homogeneous cylindrical thermal lens and avoids depolarization by birefringence. In an amplifier a confocal arrangement of two cylindrical mirrors folds the laser radiation several times through the gain volume [14,15]. Perpendicular to the pump line the thermal lens reproduces the laser mode on every roundtrip between the mirrors. In the plane of the pumped volume the beam is expanded each passage through the laser crystal by a constant factor (Fig. 2).

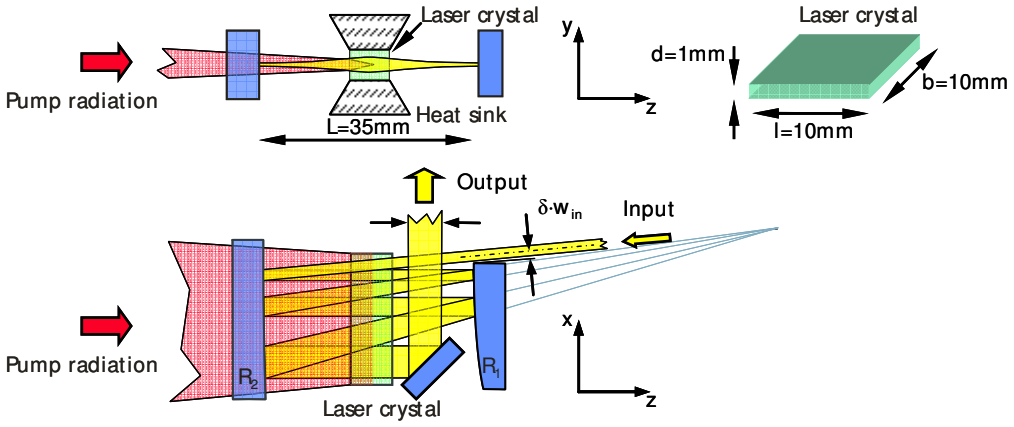

Fig. 2. Schematic setup of an Innoslab amplifier

Innoslab lasers are designed for a moderate gain of about a factor of 2 - 10 per pass. By the confocal cavity (Fig. 2) as many as 9 passes through the slab and amplification factors of 1000 are achieved. Nevertheless Innoslabs are single-pass amplifiers; at each passage a new section of the gain volume is saturated. In Innoslab lasers beam expansion on every passage through the slab balances the increase of power and intensity. This decisively improves the efficiency by homogeneous saturation of the gain medium and constantly keeps the intensity away from the damage threshold of the optical components (section 2.5).

#106480 - $15.00 USD Received 21 Jan 2009; revised 20 Apr 2009; accepted 20 Apr 2009; published 6 Jul 2009

2.3. Scaling the average power of fiber, thin-disk and Innoslab amplifiers

The common advantage of fiber, thin-disk and Innoslab lasers is the scalability of the average output power to the kilowatt level at almost diffraction limited beam quality. In fiber lasers mode area of core and cladding and the fiber length, in thin-disk lasers the diameter of the disk and in Innoslab lasers the width and length of the slab can be scaled.

2.3.1 Thermal lensing

A high transversal beam quality e.g. low optical path distortion inside the amplifier is essential for most applications. The optical surfaces have to be of high quality and the gain has to be constant across the beam. Saturation of the gain and pump intensity have to be suitably adapted. The main challenges are aberrations of the laser radiation induced by the thermal load of the gain medium. Waste power should be reduced by high laser efficiency and the thermal gradient has to be engineered to minimize aberrations of the thermal lens.

In Fiber lasers there is strong thermal lensing inside the fiber but due to the confinement inside the fiber core it has virtually no effect on the beam quality at the fiber exit [16,17]. Nearly diffraction limited output power up to 6 kW cw-radiation has been achieved [18].

In the Thin-Disk laser waste power is transported in the direction of the laser radiation to the heat sink. In the idealized case of one-dimensional heat flow and temperature gradients there is no thermal lens. To achieve best performance, the disk has to be as thin as possible to prevent radial heat flow and to minimize the temperature of the uncooled disk surface. In addition the disk acts as a mirror and has to be mounted on a well defined supporting structure. Irregular warping caused by the stack of laser crystal, HR coating and cooling device made out of different materials has to be prevented. Average output powers of 225 W transversal single-mode and multi 10 kW multi-mode cw-radiation has been demonstrated [10].

In Innoslab lasers pumping a homogeneous line along the beam path inside the slab generates a cylindrical lens (Fig. 2). The focal length of the thermal lens in y-direction can be very short. The matching cavity with a length of only a few centimeter might be challenging to engineer, but it is mechanically and optically exceptionally stable. Due to the confocal lens duct, the strong gain apertures and the small beam diameter of some 100 µm in y-direction deviations from a parabolic phase profile do not disturb the output beam quality, which is essentially diffraction limited. To avoid thermal gradients in x-direction the pump radiation has to be carefully homogenized in slow axis (see section 4). In an Innoslab amplifier the beam paths inside the laser crystal ought to overlap in x-direction as tight as possible and to be of similar intensity. As the seed laser beam is coupled in and out by spatial separation, diffraction by incomplete overlap and by mirror edges has to be balanced (section 3.3). Beam quality can be very high ($M^2 < 1.5$, section 5) at powers up to the kilowatt level [19] but distinct diffraction patterns can not be fully avoided.

2.3.2 Thermal management, pumping and mode matching

To simplify heat removal from the laser medium and the surrounding infrastructure at high average power a high laser efficiency is advantageous. For high efficiency good mode matching is essential. High pump intensities are of special importance for the high lasing threshold of quasi-three-level ytterbium doped laser materials used in high power fs-lasers. Good thermal management minimizes thermal population of the lower laser state and therefore the lasing threshold. The heat sink contact surface should be large and the distance from heat sink to heat source small.

In Fiber Lasers the excellent ratio of heat sink surface to heated volume limits temperature rise inside the core despite the low thermal conductivity of glass. In cladding pumped high power fiber lasers confinement of the pump radiation along the whole fiber length allows for high pump intensities. Adapting the ratio of the cladding to core diameter ratio efficient absorption of the pump radiation can be achieved. By recycling the transmitted pump radiation crossing the active core many times excitation can be saturated for the most part of the fiber.

#106480 - $15.00 USD Received 21 Jan 2009; revised 20 Apr 2009; accepted 20 Apr 2009; published 6 Jul 2009

Together with the perfect overlap of excited active core and guided radiation field to be amplified very high optical-optical efficiencies of $\eta_{opt} = 0.83$ can be achieved [20].

In Thin-Disk amplifiers the gain and requirements for the pump source are independent of the thickness of the disk. To maintain beam quality and thermal management by one dimensional heat flow the thickness d and thickness to diameter ratio d/D should be small. Very thin disks in the range of 100 µm maintain low temperatures inside the active medium. Output power is scaled by the mode area only. Special attention has to be paid contacting the disk to the heat sink with the dielectric coating in between. Mode matching is as good as in other end-pumped lasers, but the comparatively large beam radius on the disk requires a careful optical and mechanical cavity design.

To absorb the pump power the disk is doped as high as possible without concentration quenching [21]. Multiple passes through the disk allow efficient pump light absorption. The necessary optical expenditure additionally increases the effective pump intensity by the number of passes. Strong excitation of the laser transition with comparatively low brightness pump sources is achieved. But the gain parallel to the disk $g_{\parallel}$ is orders of magnitudes higher than the gain in the amplification beam path $g = g_{\parallel}^{d/D}$. ASE parallel to the disk substantially reduces inversion and limits the gain g for large disks. Except for low gain booster amplifiers thin disk amplifiers are used in a regenerative setup. This makes high efficiencies possible at low gain by multiple reflections of the laser radiation. But average power is limited by the power capability of the Pockels cell up to now. The attained optical efficiency $\eta_{opt} = 0.65$ [10] is comparable to fibers.

In Innoslab lasers temperature rise inside the active medium is uncritical due to the large mounting surfaces of the thin ($d \approx 1$ mm) slab soldered to the heat sink. The length l of the slab increases the contact area to the heat sink. Due to the extension l in beam propagation direction no severe restrictions by ASE exist. At constant pump power low doping and a long slab improves thermal management at constant gain at the expense of a higher required beam quality of the pump source. For high single-pass gain the slab width b should be minimized. To sustain thermal management the length of the slab l has to be scaled inversely proportional to the width b (section 3.1). That is finally limited by the beam quality of the pump source. Like in thin-disks the output power of Innoslab lasers can be scaled at constant beam quality by the width b of the slab. The height (y-dimension in Fig. 2) of the mode inside the slab stays constant and is determined by the thermal lens and therefore pump power P_p divided by slab width P_p/b only.

Mode matching in y-direction is excellent. By carefully optimizing the intensity, beam diameter and mutual overlap of the individual passes the mode matching can be very good in x-direction. Very little gain volume is unused at the edges of the slab. The line shaped pumped cross section inside the slab matches the beam characteristic of laser diode bars. Pump radiation propagates without confinement throughout the gain volume. Achieving high pump intensities along the slab still requires high brightness of the pump source. That is why Innoslab lasers were limited to neodymium doped crystals for a long time. The enormous increase in brightness and output power of commercially available diode lasers in the $\lambda_p = 940$ nm wavelength range overrode this limitation of ytterbium doped Innoslab lasers. By correct selection of the doping level, most of the pump radiation can be absorbed in a single path and simultaneously excite the whole gain volume inside the slab [22]. Excitation level is raised by double passage of the pump radiation and pumping from both sides (section 4). Optical-optical efficiencies of $\eta_{opt} = 0.48$ and slope efficiencies $\eta > 0.7$ are achieved (section 5).

2.4. Scaling the geometry of fiber, thin-disk and Innoslab amplifiers

In terms of power scalability, thermal management, beam quality and efficiency fiber, thin-disk and Innoslab are comparable. But all designs have distinct strong and weak points, which result from balancing contradictory requirements.

The (small signal) gain at constant pump power is determined by the interaction length l and the reciprocal mode area $1/A_m$ inside the active medium of an amplifier. High amplifica-

#106480 - $15.00 USD Received 21 Jan 2009; revised 20 Apr 2009; accepted 20 Apr 2009; published 6 Jul 2009

tion factors simplify the power requirements of the seed source, a strong saturated gain increases laser efficiency. A small cross section area of the active medium reduces lasing threshold and increases small signal gain, gain saturation and efficiency. At the same time the risk of damage is increased by the higher intensity of the pump- and laser radiation. In a similar manner a long interaction length increases gain, but dispersion and nonlinearity are accumulated. Due to their length and mode area the saturated single-pass gain G_{sp} and efficiency in fiber amplifiers is highest followed by Innoslab and thin-disk, but the opposite holds for damage and nonlinearity (Table 1).

The group delay dispersion and nonlinear effects like self phase modulation, stimulated Brillouin or Raman scattering can disturb or destroy the phase relation of ultrashort pulses. They have to be avoided to achieve bandwidth limited and background free high energy pulses. Nonlinearities are inverse proportional to the mode area $1/A_m$ and are accumulated on the optical path l inside an optical medium. One figure to quantify these nonlinearities is the B-integral of the accumulated self phase modulation. Normalized to the duty cycle of the ultrafast radiation to be amplified described by the quotient of peak- and average power P_{peak}/P it is a measure for the nonlinear behavior of an amplifier design. Nonlinearities in fiber amplifiers are highest followed by Innoslab and thin-disk (Table 1).

The maximum storable energy inside the laser material is determined by the mode volume V_m times the doping level or the number of laser ions. To prevent catastrophic damage by giant pulses the stored energy should be as low as possible. For a low lasing threshold e.g. high efficiency the number of laser ions should be small as well. On the other hand a large number of laser ions is advantageous to attain high pulse energies and good thermal management by a large mode volume. Normalized to the average output power thin-disk and Innoslab have comparable numbers of laser ions inside the beam path. In fibers the number is about one order of magnitude lower which is one reason for their high efficiency (Table 1). In combination with the long interaction lengths gain and ASE is high at the same time. Particular at high amplification factors and due to the large field angle of confined states inside the fiber radiation background of the amplified laser pulses can arise by ASE in propagation direction.

Table 1. Typical dimensions of the gain volume for sub-ps fiber [23], thin-disk [11] and Innoslab amplifiers

Design	Output power P	Single-pass gain G_{sp}	Length l	Cross section (A)	Mode area A_m	Mode Volume V_m	Total B-integral $B/(P_{peak}/P)$
Fiber	145W	1000	1.2 m	∅ 80 µm	$4\cdot10^{-3}$ mm^2	6 mm^3	$1\cdot10^{-3}$
Thin-disk	18W	1.08	115 µm	∅ 1.3 mm	0.5 mm^2	0.15 mm^3	~$5\cdot10^{-6}$
Innoslab	400W	10	10 mm	0.2 x 10 mm^2	0.04...1 mm^2	20 mm^3	$2\cdot10^{-5}$

2.5. Scaling the peak power of fiber, thin-disk and Innoslab amplifiers

In *Fiber amplifiers* the mode area is constantly increasing by simultaneously shortening fiber length to increase pulse energy without damage and pulse degradation by nonlinear effects [8,23]. In principle the requirements for the pump source do not depend on the fiber length and by that on the gain. But to absorb the pump power in very short fibers the ratio of pump cladding diameter to active core diameter should be small, requiring bright pump sources. Large fiber cores makes handling of the fiber, thermal management and supporting fundamental mode radiation more and more difficult, reducing the simplicity of fiber lasers [16,17,24]. Besides these efforts the B-integral in fibers is usually far beyond the critical value for filamentation of $B \approx 3$, prevented by the optical confinement of the fiber only. By that the ultimate peak power inside fibers remains limited ($P_{max} \approx 1.84 \cdot P_{crit} = 4$ MW, silica) by catastrophic self focusing only, independent of the mode area inside the fiber [25].

#106480 - $15.00 USD Received 21 Jan 2009; revised 20 Apr 2009; accepted 20 Apr 2009; published 6 Jul 2009

In Thin Disk amplifiers the optical path inside the Pockels cell of the regenerative setup is two orders of magnitude longer than the disk. Therefore it is the main source for dispersion and nonlinearities limiting not only average but also maximum peak power during amplification. By large beam cross sections inside the Pockels cell nonlinear effects can be reduced. But dimensions of the Pockels cell are limited and a large beam diameter increases alignment sensitivity of the cavity. To overcome losses (e.g. Pockels cell) and to minimize nonlinearity by fewer roundtrips high gain by a small mode area is desirable for a simple setup. Good beam quality and thermal management by large, thin disks and high gain and reduced nonlinearity by small thick disks have to be weighed up. Nevertheless regenerative thin-disk amplifiers exhibit the lowest nonlinearity of ultrafast amplifiers at moderate powers (Table 1) and almost negligible nonlinearity in low gain high power multi-pass booster amplifiers.

In Innoslab amplifiers high gain, high efficiencies and high damage threshold are combined by matching the beam cross section to the power of the amplified laser radiation by beam expansion inside the cavity. By a short interaction length inside the laser material and by keeping the ratio of laser- to saturation intensity constant the nonlinearity is minimized. The low nonlinearity (Table 1) of the single-pass setup is one of the key advantages of Innoslab amplifiers. In thin-disk amplifiers this requires a regenerative setup. In fiber and thin-disk booster amplifiers this has to be realized in discrete sequential amplification stages. Due to the geometry in Innoslab lasers ASE inside the slab is very low. By the surrounding open unstable cavity ASE is increased only in small fraction of space angle and background of the amplified radiation is very small. Feedback by diffraction at the mirror edges of the unstable resonator can support parasitic oscillations. As they are tilted in some angle to the beam path of the amplifier additional background radiation cannot arise but they limit the maximum amplification factor.

The chirped pulse amplification (CPA) of ultra short laser pulses is an established technology to avoid damage and pulse distortion by nonlinear effects at amplification [7]. To attain high stretching factors up to the nanosecond level free space grating setups have to be used. For high power applications conventional reflective gratings are not applicable. Dielectric reflection gratings and transmissive silica diffraction gratings which can handle very high average powers >8 kW are available recently. In particular a compressor for several 100 W average power is a considerable additional operating expense. In fiber amplifiers CPA has to be applied always, adding to their complexity. In present picosecond thin-disk amplifiers CPA can be avoided at repetition rates above some 100 kHz due to the large beam cross sections even though the integrated Pockels cell exhibits a high nonlinearity. In Innoslab amplifiers above ~10 MHz repetition rate no CPA is necessary. Due to the small amount of material in the beam path almost transform limited femtosecond pulses without additional compression are achieved. With CPA the repetition rate of Innoslab amplifiers can be scaled down like in thin-disk lasers to about 10 kHz without limitations by nonlinear distortions, damage or efficiency.

Table 2. Design specific features of thin-disk, fiber and Innoslab amplifiers

	Fiber	Innoslab	Thin-disk	
	1W-1000W	100W-1000W	regenerative <100W	multi-pass >>100W
Fundamental mode avg. power	++	+	++	
Amplification factor	++	+	+	−−
Average power scaling	++	+	−	++
Pulse energy	−−	+	+	++
Nonlinearity	−−	+	+	++
Dispersion	−−	+	−	++

#106480 - $15.00 USD Received 21 Jan 2009; revised 20 Apr 2009; accepted 20 Apr 2009; published 6 Jul 2009

In summary fiber, thin-disk and Innoslab amplifiers are evenly matched in terms of scalability, beam quality and efficiency. In detail fiber and thin-disk have essential strong and weak points like single-pass gain and nonlinearity due to the very different beam cross sections (Table 2). At high amplification factors at intermediate power and high repetition rates fiber amplifiers and at very high powers thin-disk amplifiers cannot be surpassed. The big advantage of the Innoslab amplifier is the position between these two designs without severe weaknesses due to the intermediate beam cross section and the design specific beam expansion during amplification.

3. Numerical optimization

3.1. Conception

For high gain, low lasing threshold and good thermal management Yb:YAG has been selected as laser material. By numerical optimization efficiency and beam quality are maximized and B-integral minimized. To achieve $P > 300\,\mathrm{W}$ output power a pump power of $P_p = 800\,\mathrm{W}$ has been estimated. For a low lasing threshold and high efficiency an intensity well above the saturation intensity $I_{sat}(\lambda_p) = 28\,\mathrm{kWcm^{-2}}$ [4] of the pump radiation has to be guaranteed. Laser radiation is absorbed in unpumped regions otherwise. The highest possible brightness of the pump radiation and matching the beam parameters of the pump source to the mode volume inside the slab crystal is essential for the performance of an ytterbium based Innoslab.

The two commercially available horizontal laser diode stacks (JOLD-408-HSC-4L) used in our setup consist of four collimated laser diode bars each. They provide up to 480 W in a $46 \times 0.8\,\mathrm{mm^2}$ aperture with $150 \times 4\,\mathrm{mrad^2}$ far field divergence. To focus the pump radiation into the slab a beam forming optics was designed, containing a wave guide for beam homogenization of the laser diodes in slow axis [13]. Only a slight beam degradation and homogeneous intensity distribution in slow axis, diffraction limited imaging of the collimated laser diodes in fast axis and a double pass throughout the slab are realized. Diffraction limited pump radiation in fast axis is focused to a line of 10 mm width and $2w_p = 200\,\mu\mathrm{m}$ height over 10 mm Rayleigh length inside the YAG crystal or $2w_p = 150\,\mu\mathrm{m}$ at $z_R = 5\,\mathrm{mm}$. The cylindrical thermal lens inside the slab is estimated by one-dimensional heat flow out of the homogeneous pumped $2w_p = 200\,\mu\mathrm{m}$ thick volume by $f_{th} = \lambda \cdot b \cdot 2w_p / \chi \cdot \eta_h \cdot P_{abs}$ (Yb:YAG; $\chi = 1 \cdot 10^{-5}\,\mathrm{K^{-1}}$ [5]; $\lambda = 8.6\,\mathrm{Wm^{-1}K^{-1}}$ [26]; $\eta_h = 0.1$ [27]) to $f_{th} = 25\,\mathrm{mm}$ focal length at $2w_p = 200\,\mu\mathrm{m}$ and $f_{th} = 18\,\mathrm{mm}$ at $2w_p = 150\,\mu\mathrm{m}$ respectively. In the second case a cavity length too small to engineer is required for reproducing a cavity mode on every roundtrip, which is matched to the gain volume in fast axis (y-direction, Fig. 2). Therefore a focal line of $2w_p = 200\,\mu\mathrm{m}$ height inside a slab of width $b = 10\,\mathrm{mm}$ was chosen.

The thickness d of the slab influences the temperature rise inside the slab and the fracture limit by thermal stress and has to be as small as possible. For simple handling a slab thickness $d \approx 1\,\mathrm{mm}$ is practical. The slab length l determines the absolute temperature rise and fracture limit by the area of heat removal. By soldering the slab to the actively cooled heat sink, the surface temperature is kept constant and temperature rise by one-dimensional heat flow can be calculated to $\Delta T = \eta_h \cdot P_{abs} \cdot (h - w_p) / (4 \cdot \lambda \cdot l \cdot b)$ ($\Delta T = 18\,\mathrm{K}$, $l = b = 10\,\mathrm{mm}$; $d = 1\,\mathrm{mm}$). Thermal stress was calculated by the finite element method. In summary heat removal can easily be achieved and stress is no limitation, so a slab of $l = 10\,\mathrm{mm}$ length is used. At a focal line width $2w_p = 200\,\mu\mathrm{m}$ requirements on the pump beam quality of the fast axis are reduced to $M_y^2 = 10$.

While the basic setup of the amplifier is straight forward, final optimization is done by modeling inversion and beam propagation in three dimensions. The independent parameters to optimize efficiency and beam quality are doping of the laser crystal, number of roundtrips N, length L and magnification M of the confocal cavity, distance between beam center and diffracting edges at input-/output coupling $\delta \cdot w$ and beam parameters q_s of seed radiation. Correct doping level guarantees absorption of the pump radiation and inversion along the crystal length at the same time. The number of roundtrips has to balance total gain, saturation and B-integral. The cavity length together with thermal lens and gain guiding determines mode matching in fast axis (y-direction). The remaining parameters are used to maximize mode area

#106480 - $15.00 USD Received 21 Jan 2009; revised 20 Apr 2009; accepted 20 Apr 2009; published 6 Jul 2009

and beam overlap in slow axis (x-direction) in order to minimize B-integral and peak intensities and to maximize beam quality and efficiency.

3.2. Numeric

To consider the quasi-three-level behavior of ytterbium the rate Eqs. are solved in three dimensions for the static case following a procedure by Bourdet [28]:

$$\frac{1}{\alpha_p L} I_p \left(1-\exp\left(\alpha_p \left(\beta - f_p\right)L\right)\right)+\frac{1}{\alpha_l L} I_l \left(1-\exp\left(\alpha_l \left(\beta - f_l\right)L\right)\right)-\beta = 0 \qquad (1)$$

$$G = \exp\left(\alpha_l \left(\beta - f_l\right)L\right),\ \ \Gamma = \exp\left(\alpha_p \left(\beta - f_p\right)L\right) \qquad (2)$$

I_p and I_l are the intensities of pump and laser radiation respectively normalized on their specific saturation intensities, α_p and α_l are absorption coefficients, f_p and f_l are temperature population numbers for a quasi-three-level scheme, L is the thickness of the crystal gain sheet. β is the inversion parameter, i.e. the relative occupation of the upper manifold of the Yb^{3+} energy levels. Eq. (1) is implicit and can be solved for β by Newton's method. Gain G and absorption Γ are calculated from Eq. (2). Eq. (1) can be derived by the rate Eq. in a volume with length L in the static case. This different representation to [28] shows clearly the symmetry of pump and laser radiation. Depending on the ratio of inversion parameter β and f radiation is absorbed or amplified ($f_l = 0.07; f_p = 0.78$ at 300 K).

The gain results from the rate Eq. depending on intensities of the propagating pump- and laser radiation again depending on the gain G and absorption Γ. Therefore gain and propagating laser fields are calculated in the static case in a recursive manner. The pump radiation is propagated by ray tracing. The amplified electric field is numerically propagated by two different numerical approaches. For this purpose the slab crystal is split up into 10-20 gain- and phase-sheets and the radiation fields are propagated in between.

The first method is mode expansion of the electrical field as a simple and accurate approach to propagate almost transform limited radiation fields. In fast axis only a Gaussian beam is propagated, gain and thermal lens are represented by complex matrices. In slow axis the beam is expanded in Hermitian modes up to the 10^{th} order, which are separately propagated by matrices and recombined considering the different Guoy phase shifts. The second method applied is solving the Fresnel Huygens diffraction integral. Arbitrarily distributed electromagnetic fields can be propagated in this case. The integrals are solved by Fast Fourier Transformation. Sheets with $2^7 \times 2^{11}$ base points represent the gain, phase and field amplitude. Due to the propagation of nearly diffraction limited radiation the electrical field is exactly propagated to the next sheet without breaking the Nyquist criterion. By the second kind of propagation even complex fields caused by diaphragms like the mirror- and slab edges at in- and output coupling can be propagated.

Propagation in fast axis is determined by thermal lens, gain guiding and plane mirrors in y-direction separated by a distance L. The beam path is optimized by finding the self consistent solution. Propagation in slow axis is determined by magnification of the confocal cavity $M = R_1/R_2$, length $L = (R_1+R_2)/2$ (mirrors with radii of curvature R_1, R_2 in x-direction) and the geometric and complex beam parameters α_{in}, x_{in} and q_{in}. The beam path is optimized analytically by spreading the beam path inside the slab and moving and tilting the cavity mirrors to force a safety distance $\delta \cdot w$ of the beam of radius w at mirror- and slab edges (Fig. 2). At the same time the B-integral is minimized by maximizing the output beam diameter $2w_{out}$.

3.3. Optimization

A tight overlap of the beam passes inside the slab crystal and a wide separation of the beams at the edges of the mirror in case of in- and output coupling are opposing requirements. A high overlap in the slab crystal yields an even intensity distribution and saturation of the pumped volume (Fig. 3). This maximizes extraction efficiency and prevents rising of the

#106480 - $15.00 USD Received 21 Jan 2009; revised 20 Apr 2009; accepted 20 Apr 2009; published 6 Jul 2009

intensity at the edges of the beam, which reduces the beam quality. On the other hand a large safety distance $\delta \cdot w$ or security factor δ (Fig. 2) improves beam quality by reducing diffraction at the mirror edges. In order to find a trade-off the seed beam parameters have been calculated for different security factors δ_{out} at the slab edge and output coupling mirror ((b) and (c) in Fig. 3). The security factor at the input coupling mirror is kept at $\delta_{in} = 2.0$ ((a) in Fig. 3).

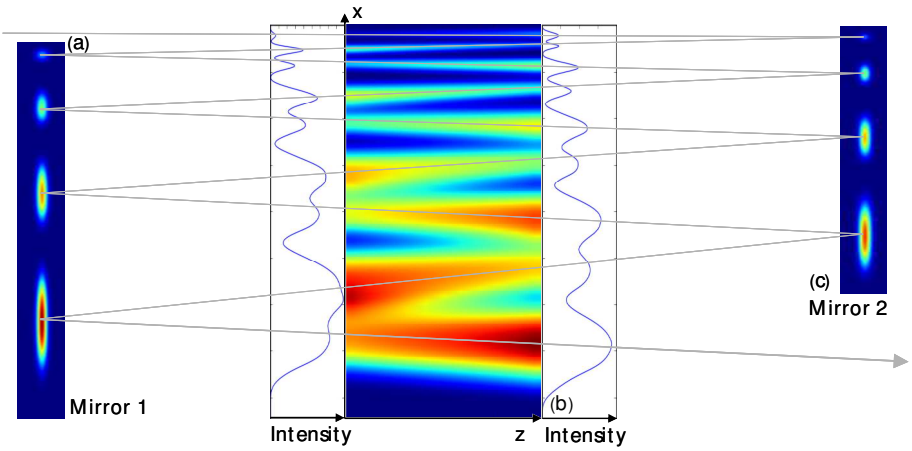

Fig. 3. Calculated 3dim. intensity distribution in the crystal and on the mirrors. The beam has to pass the edges of mirror 1 (a), crystal (b) and mirror 2 (c) with sufficient safety distance δ.

For beam propagation inside the amplifier a security factor δ_0 was forced without amplification. Because the beam is influenced by gain guiding depending on the overlap and inversion inside the crystal the actual security factor δ differs from δ_0. For a high security factor δ_0 the beam is slim inside the slab and the B-integral is increased at the same time (Fig. 4(b)).

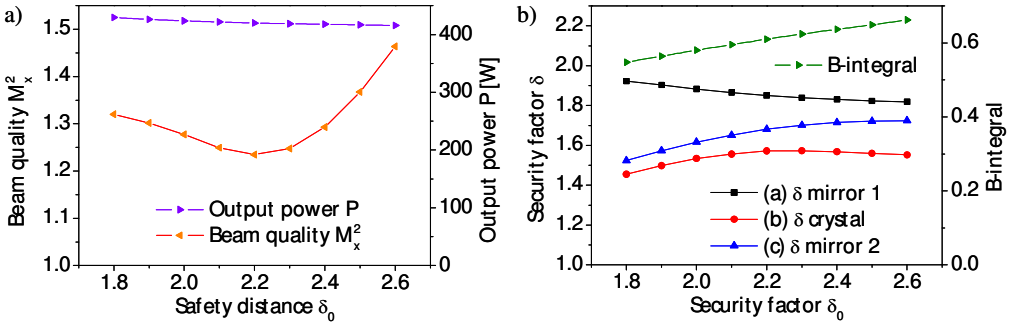

Fig. 4. Simulation of the amplifier for different seed beam parameters obtained for different security factors δ_0 ($P_P = 800$ W, $P_S = 3$ W, 9 passes, $M = 1.4$).

The unsaturated gain at the edges of the beam by the diminished overlap in the crystal increases beam radius and reduces beam quality. This is why the safety distances in Fig. 4(b) are limited. The best compromise of output power, B-integral and beam quality is achieved for a security factor $\delta_0 = 2.2$ (Fig. 4(a)). This optimization slightly depends on seed and pump power, magnification of the confocal cavity and number of passes.

To optimize the confocal cavity the magnification M was varied from $M = 1$ (plane mirrors) to $M = 2$. In the simulation for each magnification the seed beam parameters and mirror angles determining beam propagation inside the amplifier are optimized in the way described above. There is a strong minimum at $M = 1.6$ for beam quality M^2, while the output power changes only slightly (Fig. 5(a)). The occurring peak intensities decrease with magnification, as the beam radius at the last crystal pass increases. For small magnifications beam radius and intensity increase every passage through the crystal (Fig. 3; $M = 1.4$).

#106480 - $15.00 USD Received 21 Jan 2009; revised 20 Apr 2009; accepted 20 Apr 2009; published 6 Jul 2009

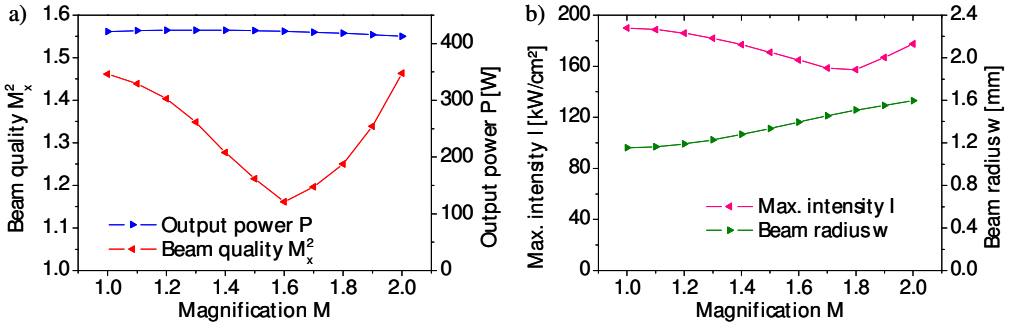

Fig. 5. Output power and beam quality (a), peak intensity and beam radius of the last pass through the crystal (b) for different magnifications ($P_P = 800$ W, $P_S = 3$ W, 9 passes).

For higher magnifications the beam radius decreases first, before it expands after the third or fourth pass. The peak intensity of the smallest beam gets higher than at the last pass for magnifications $M > 1.8$ (Fig. 5(b)). The B-integral is virtually independent of the magnification. This optimization depends on seed and pump power and number of passes through the crystal.

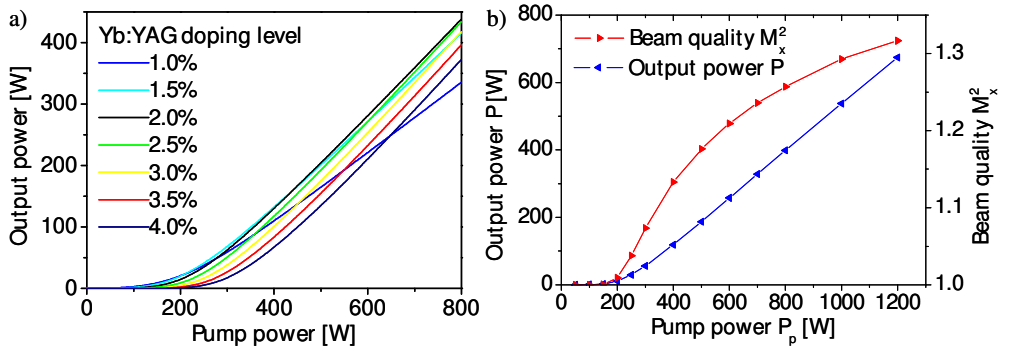

Fig. 6. Calculated output power at various doping levels (a) and output power and beam quality M^2 in slow direction versus pump power for the Yb:YAG amplifier in section 4 seeded by $P_S = 1$ W at $\lambda_S = 1030$ nm, $M = 1.4$, $\lambda_p = 940$nm.

Low doping levels correspond to a low lasing threshold. Higher doping levels result in a higher slope efficiency at the expense of a higher lasing threshold. The output power over the pump power has been calculated for different doping levels of the Yb:YAG crystal. For a pump power of 800 W output power is highest for a doping level of 2% (Fig. 6(a)). For doping levels >2% pump power is almost completely absorbed inside the crystal and the slope efficiency stays constant.

In the experiments a confocal cavity of magnification $M = 1.4$ was seeded by a round beam of equal beam parameters in slow- and fast-axis. The power characteristics and beam quality in slow axis was calculated for optimized seed beam parameters and cavity (Fig. 6(b)). Temperature inside the crystal and thermal lens were scaled with pump power. Temperature dependence of the cross sections is taken into account [29, 30]. In fast direction gain guiding is strong and beam quality is diffraction limited ($M_y^2 < 1.01$; $P_P > 300$ W). The beam parameters of the output beam vary slightly with absorbed pump power due to the variable focal length of the thermal lens. Aberrations of the thermal lens are not considered.

4. Setup

Two horizontal stacks of four collimated laser diode bars (JOLD-408-HSC-4L) provide up to 480 W at $\lambda_p = 940$ nm each. The radiation is imaged into a planar waveguide for homogenization in slow axis. Afterwards the exit of the waveguide is imaged by a relay optic into the

#106480 - $15.00 USD Received 21 Jan 2009; revised 20 Apr 2009; accepted 20 Apr 2009; published 6 Jul 2009

1x10x10 mm^3 Yb:YAG (2% doping level). In fast axis the collimated laser diode bars are imaged into the middle of the slab, adapting beam parameters by two cylindrical lenses. By this procedure the beam profile inside the slab is almost independent of the collimation of the diode lasers. Smile or misalignment of the fast axis collimation only slightly broadens the focal line inside the slab crystal.

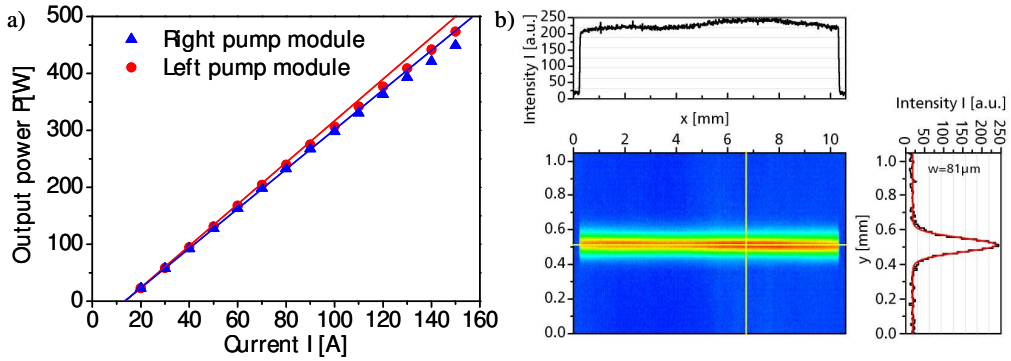

Fig. 7. Power characteristic of pump-modules (a) and beam profile of left pump (b)

For both pump modules a focal line width of $2w_p = 162\,\mu m$ and $2w_p = 192\,\mu m$ at $z_R = 8.5$ mm Rayleigh length are measured (Fig. 7). The transmission of the pump module optics at full power of $P_P = 449$ W and $P_P = 474$ W at 150 A exceeds 90%. Making use of the polarization of the laser diodes the transmitted pump power is imaged back telecentrically into the slab. In double pass ~90% of the pump radiation is absorbed.

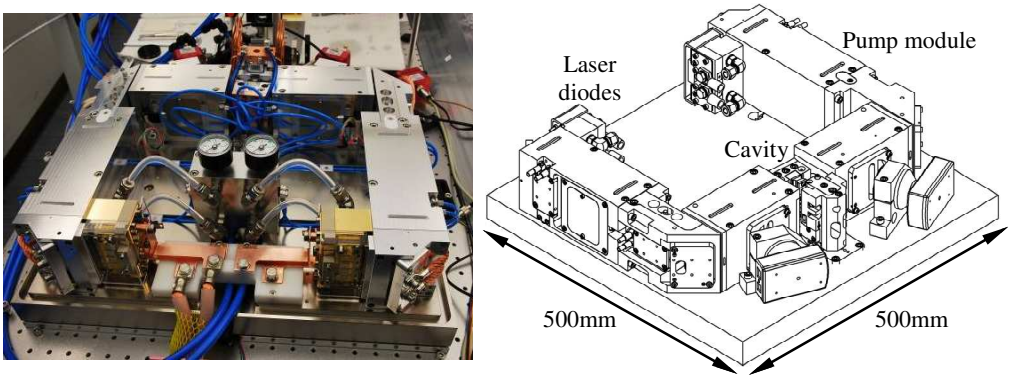

Fig. 8. Amplifier setup

The two pump modules enclose the cavity of the amplifier in Fig. 8. The confocal cavity of magnification M=1.4 consists of two cylindrical mirrors and two plane dichroic folding mirrors. Due to the cavity length of 35 mm it is very compact and stable. Temperature stabilization by water cooling of the whole setup ensures stable longtime operation.

The amplifier was seeded by a 460 x 200 x 80 mm^3 sized Yb:KGW oscillator (HighQ Laser Innovation GmbH) of $P_S = 2.5$ W output power at 75.8 MHz, matching the compact dimensions 500 x 500 x 150 mm^3 of the amplifier (Fig. 8). The nearly transform limited $\tau = 316$ fs pulses of $\Delta\lambda = 3.7$ nm bandwidth are centered at $\lambda_s = 1029.4$ nm (Fig. 10). For comparison we used a home build Yb:YAG cw-oscillator with up to 12 W output power at $\lambda_s = 1029.8$ nm. The circular and non-stretched seed radiation of both oscillators passes the gain volume nine times before extraction.

#106480 - $15.00 USD Received 21 Jan 2009; revised 20 Apr 2009; accepted 20 Apr 2009; published 6 Jul 2009

5. Results

In a first experiment the amplifier has been seeded with a Yb:YAG oscillator operated in continuous wave operation at $\lambda_s = 1029.8$ nm. Up to $P = 389$ W output power at $P_p = 771$ W pump- and $P_s = 4$ W seed power has been achieved. Above a threshold pump power of 250 W a slope efficiency $\eta > 0.7$ is attained. Starting parasitic oscillations of the cavity limit the amplification factor to $G \approx 1000$. Output power is only limited by the wavelength shift of the laser diodes away from the highest absorption of Yb:YAG at 940 nm wavelength, decreasing absorbed power at $P_p > 771$ W. Apart from this the measured amplification is in good agreement to the calculated lines in Fig. 9.

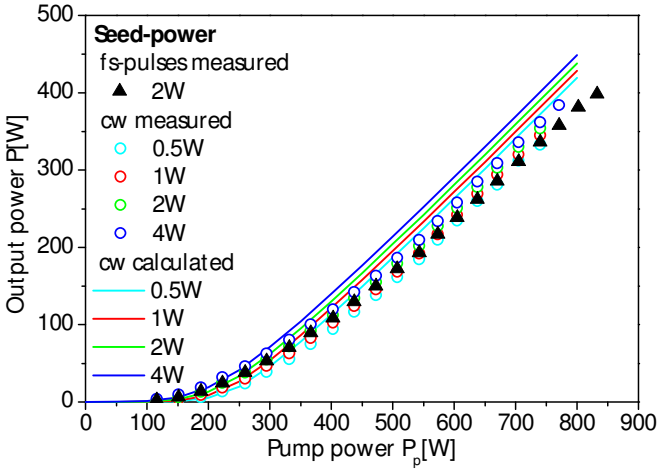

Fig. 9. Measured and calculated output power of the amplifier seeded by cw- and fs-oscillators.

For the short pulse experiments we seeded the amplifier with the Yb:KGW fs-oscillator. Only a spherical telescope and a focusing lens were used for mode matching to the amplifier mode. No stretcher or cylindrical beam transformation were employed. An optical isolator was used to protect the oscillator against feedback by the amplifier. Measurements without isolator left all results unchanged. Up to $P = 400$ W of linearly polarized fs-radiation was extracted from the amplifier (Fig. 9) at $P_s = 2$ W seed power and 2x135 A diode current corresponding to $P_P = 833$ W pump power. To increase absorbed pump power we decreased water temperature of the laser diodes by 4°C. After nine passes inside the 10 mm long laser crystal the pulses of $\tau = 682$ fs duration (FWHM, sech^2-fit) stay nearly transform limited ($\tau\Delta\nu = 0.348$) without compression (Fig. 10). At 75.8 MHz repetition rate and pulse energies of $E = 5.3$ µJ no sign of self phase modulation is visible. Gain narrowing reduces the spectral bandwidth $\Delta\lambda_s =$ 3.7 nm of the oscillator to $\Delta\lambda = 1.81$ nm behind the amplifier (Fig. 10).

After amplification a cylindrical telescope transforms the radiation into a circular beam. Beam quality was measured (Spiricon M^2-200/v.4.2, 2nd momentum method) to be $M_x^2 = 1.44$ and $M_y^2 = 1.28$ respectively at $P = 400$ W output power (Fig. 11(a)). The remaining astigmatism is due to the variable cylindrical thermal lens, which was completely compensated at $P =$ 200 W. The RF spectrum measured by a photodiode is noise free down to 10 Hz (60 dB) (Fig. 11(b)). There is no sign of background radiation or nonlinear spectral broadening. Lasing of the amplifier is completely suppressed by the seed radiation at seed powers as low as $P_s = 680$ mW and $P = 380$ W output power. The amplifier is seeded inside the amplification bandwidth by 340 mW resulting in an amplification factor exceeding G = 1000.

#106480 - $15.00 USD Received 21 Jan 2009; revised 20 Apr 2009; accepted 20 Apr 2009; published 6 Jul 2009

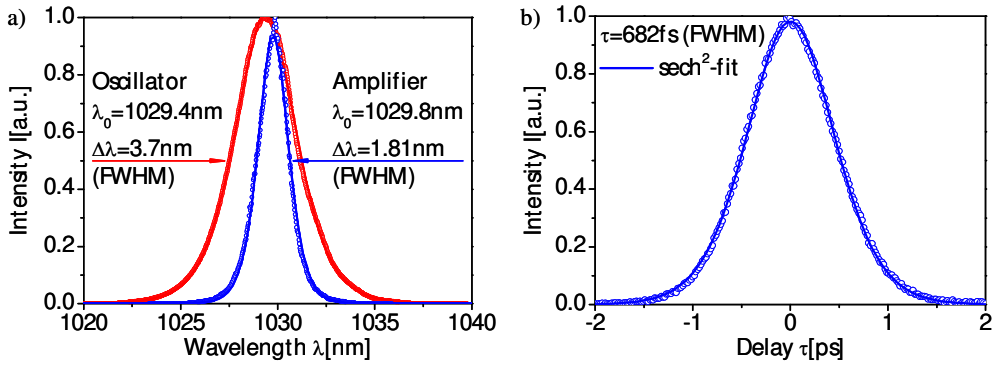

Fig. 10. Spectra (a) and autocorrelation (b) fitted by sech^2 of fs-oscillator (red) and amplifier (blue) at $P = 400$W output power

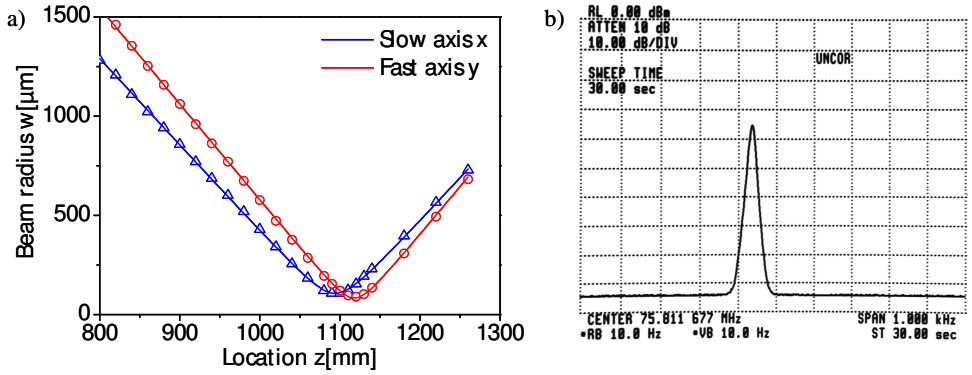

Fig. 11. Beam radius (a) and amplitude noise (b) at $P_{out} = 400$ W output power

6. Scaling power, pulse energy and bandwidth

At the present repetition rate of 76 MHz there are no indications of limitations of the described Yb:YAG Innoslab amplifier. At a pulse energy $E_p = 5.2\,\mu$J and pulse duration $\tau = 700$ fs the B-integral was calculated to $B = 0.42$ and the peak intensity on the surfaces of the crystal to $I_{peak} = 2.4$ GWcm^{-2}. With a suitable seed source pulse energies of $E_p = 40\,\mu$J at 10 MHz repetition rate should be attainable without chirped pulse amplification (CPA). Taking nonlinear effects and damage thresholds into account, with CPA some 10 mJ at >10 kHz repetition rate are expected to be feasible. Lower repetition rates or pulsed pumping will not gain technical advantages, as heat removal is not limiting the performance. By cascading two or three amplifiers1 kW average power at $E_p = 100$ mJ with and $E_p = 100\,\mu$J without CPA are feasible. Reduced number of passages in the first stage and one or two passages in the following stages keeps B-integral under control.

With new and brighter laser diode bars emerging, the output power of a single amplifier head can be further improved. Thermal management allows for about 50% further increase. But brighter or more powerful diode lasers can considerably simplify the number of optics in the pump modules as well.

#106480 - $15.00 USD Received 21 Jan 2009; revised 20 Apr 2009; accepted 20 Apr 2009; published 6 Jul 2009

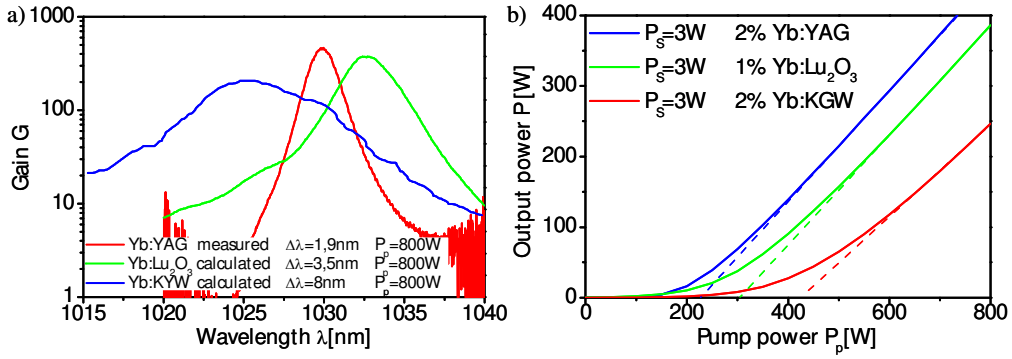

Fig. 12. Calculated saturated and unsaturated (dashed) Gain of an Innoslab amplifier based on different laser materials versus pump power (a) and wavelength (b)

Until now only Yb:YAG was examined as the gain medium due to its superior gain and thermal properties. Other laser materials like Yb:KGW promise an increase of the gain bandwidth by a factor of four (Fig. 12(a)). Mechanical durability was already proved at full pump power. In spite of the three times lower heat conductivity the thermal management is expected to be sufficient. But due to the lower gain cross section lasing threshold is higher and output power considerably lower than for Yb:YAG (Fig. 12(b)). The rarely used Yb:Lu_2O_3 having comparable heat conductivity to Yb:YAG may be an intermediate candidate for higher gain bandwidth.

7. Conclusion

At high average power, Innoslab amplifiers bridge the gap between fiber amplifiers with high single-pass gain but high nonlinearities, small cross section and damage threshold and thin-disk amplifiers with large cross sections but low single-pass gain. The ultimate high average and peak power ultrafast laser probably utilizes a fiber oscillator and preamplifier to reach the Watt level, an Innoslab for amplification to the multi 100 W level and a thin-disk multi-pass amplifier for attaining the multi kW level at nearly diffraction limited beam quality.

Acknowledgments

The authors thank Anne-Laure Calendron, Joachim Meier and Max Lederer of HighQ Laser Innovation GmbH, Austria for assistance and providing the oscillator. This work was supported by Federal Ministry of Education and Research, contract 13N8717.

#106480 - $15.00 USD Received 21 Jan 2009; revised 20 Apr 2009; accepted 20 Apr 2009; published 6 Jul 2009